A comparison of resting-state brain activity in humans and chimpanzees

James K. Rilling*[†‡§¶], Sarah K. Barks*[‡], Lisa A. Parr[†‡§], Todd M. Preuss[†‖]**, Tracy L. Faber[††], Giuseppe Pagnoni[§], J. Douglas Bremner[§†††‡‡], and John R. Votaw[†††‡‡]

*Department of Anthropology, Centers for [†]Behavioral Neuroscience and [‡‡]Positron Emission Tomography, Divisions of [‡]Psychobiology and [‖]Neuroscience, Yerkes National Primate Research Center, and Departments of [§]Psychiatry and Behavioral Sciences, **Pathology, and [††]Radiology, Emory University School of Medicine, Emory University, Atlanta, GA 30322

Edited by Marcus E. Raichle, Washington University School of Medicine, St. Louis, MO, and approved September 6, 2007 (received for review May 31, 2007)

In humans, the wakeful resting condition is characterized by a default mode of brain function involving high levels of activity within a functionally connected network of brain regions. This network has recently been implicated in mental self-projection into the past, the future, or another individual's perspective. Here we use [^{18}F]-fluorodeoxyglucose positron emission tomography imaging to assess resting-state brain activity in our closest living relative, the chimpanzee, as a potential window onto their mental world and compare these results with those of a human sample. We find that, like humans, chimpanzees show high levels of activity within default mode areas, including medial prefrontal and medial parietal cortex. Chimpanzees differ from our human sample in showing higher levels of activity in ventromedial prefrontal cortex and lower levels of activity in left-sided cortical areas involved in language and conceptual processing in humans. Our results raise the possibility that the resting state of chimpanzees involves emotionally laden episodic memory retrieval and some level of mental self-projection, albeit in the absence of language and conceptual processing.

comparative cognition | neuroimaging | default mode

Human resting-state cognition is thought to involve freely wandering past recollections, planning for the future, inner speech, and simulation of behavior (1–3). Recently, cognitive neuroscientists have turned their attention to elucidating the neural bases of human resting-state cognition. A metaanalysis of functional brain imaging studies showed that several brain regions consistently deactivate in a variety of attention-demanding cognitive tasks (4), implying they may be tonically active at rest. These areas overlap considerably with regions showing the highest level of blood flow and metabolism at rest (5). These two observations led to the default-mode hypothesis, which posits the existence of an organized mode of brain function present as a baseline or default state and attenuated during specific goal-directed tasks (5). Gusnard and Raichle (6) partitioned the default mode regions into four general groups on the basis of anatomical location: (*i*) posterior medial cortices, including the precuneus, posterior cingulate, and retrosplenial cortices, that have been implicated in self-related episodic memory retrieval (7); (*ii*) posterior lateral cortices, including Brodmann's area (BA) 39, 40, 22, and 19, that are related to conscious awareness (6) but also semantic or conceptual processing (8); (*iii*) ventral medial prefrontal cortex (MPFC), thought to be involved in emotional processing that guides decision-making (9); and (*iv*) finally, dorsomedial PFC, which is proposed to mediate self-referential mental activity and mental-state reflection (10, 11). Subsequent functional MRI studies demonstrated that this set of areas is functionally connected at rest, indicating they constitute a network across which activity increases or decreases in unison (12–14).

The mental life of our closest living relative, the chimpanzee, is known to us only through inferences based on behavior. Is it possible that, like humans, the chimpanzee default mode of brain function at rest involves the retrieval of self-related episodic memories, possibly including reflection on mental states? In contrast to most other primates, chimpanzees are capable of recognizing themselves in mirrors (15), suggesting they may have the prerequisite self-concept that introspection would require. There has been considerable debate as to whether chimpanzees can make inferences about the mental states of others. Anecdotal evidence of deception in field studies raises the possibility that they can (16); however, this has been difficult to definitively demonstrate in experimentally controlled laboratory studies (compare, e.g., refs. 17 and 18). As this debate continues, we offer an additional source of evidence in the form of functional brain imaging. We use functional neuroimaging to define resting-state brain activity in chimpanzees as a potential window onto their mental world, and we compare these results with those of a human sample.

Central to this study is the use of [^{18}F]-fluorodeoxyglucose (FDG) positron emission tomography (PET) ([^{18}F]-FDG PET) imaging, which makes it possible to image resting-state brain activity in awake subjects outside the scanner. Adult humans (n = 8) and adult chimpanzees (n = 5) received a dose of [^{18}F]-FDG, a radioactively labeled chemically modified glucose molecule. After entering the bloodstream, [^{18}F]-FDG accumulates and becomes trapped in neurons at a rate proportional to their glucose metabolic rate (19). During this extended period of cellular [^{18}F]-FDG uptake (≈45 min in humans and 75 min in chimpanzees), human subjects rested quietly by themselves in a private room adjacent to the PET scanner, and chimpanzee subjects rested quietly in their home cages. After the uptake period, subjects received a PET scan to image the distribution of [^{18}F]-FDG in the brain. Variation across the brain in the resulting image results from regional differences in glucose metabolism during the period of [^{18}F]-FDG uptake. Human subjects were scanned awake, whereas chimpanzee subjects were sedated and scanned in the anesthetized state. It is important to recognize, however, that because [^{18}F]-FDG uptake is largely complete before sedation, and because it leaves cells at a very slow rate, the resulting images reflect brain metabolism during the uptake period when the animal was awake and not real-time activity in the anesthetized state.

Although the homologies of chimpanzee and human cortical areas, in some cases, have not been definitively established, we

Author contributions: J.K.R., L.A.P., and T.M.P. designed research; J.K.R., S.K.B., L.A.P., J.D.B., and J.R.V. performed research; T.L.F. contributed new reagents/analytic tools; J.K.R., S.K.B., and G.P. analyzed data; and J.K.R. and T.M.P. wrote the paper.

The authors declare no conflict of interest.

This article is a PNAS Direct Submission.

Abbreviations: FDG, [^{18}F]-fluorodeoxyglucose; PET, positron emission tomography; BA, Brodmann's area; PFC, prefrontal cortex; MPFC, medial PFC.

¶To whom correspondence should be addressed. E-mail: jrillin@emory.edu.

This article contains supporting information online at www.pnas.org/cgi/content/full/0705132104/DC1.

reason that if the chimpanzee pattern of resting brain activity differs substantially from that found in humans, it is unlikely that they are engaged in the same mental processes as humans at rest. On the other hand, if chimpanzee and human patterns of activation are similar, one possible explanation is that there are similarities in their resting-state cognition.

Results

Behavioral Results. For four of the five chimpanzee subjects, cagemates were present during the [^{18}F]-FDG uptake period (see *Materials and Methods*). Analysis of videotapes of the [^{18}F]-FDG uptake period for chimpanzees showed these four animals spent no time in physical contact with their cagemate. The fifth animal was outside the camera field of view for 94% of the uptake period. However, this subject was alone during the [^{18}F]-FDG uptake period, so physical contact with the cagemate was impossible. Of the four subjects with complete video data, three spent the vast majority of the period lying down (71%, 95%, and 73%, respectively), as opposed to standing, sitting, or moving. The fourth spent the majority of the time sitting (83%). We also attempted to characterize each animal's attentional state during the uptake period. Animals were categorized as either watching, alert, neutral, or moving [definitions provided in supporting information (SI) Table 1], with neutral considered to be most closely approximate to a resting state. It was not always possible to evaluate the subject's attentional state, because they would occasionally move behind a barrel or turn away from the camera. With this caveat in mind, all four animals spent the majority of the time they were visible in the neutral state (60%, 78%, 72%, and 66%). For the remaining subject without complete video data, it could be inferred he did not move from the limited area of the camera's blindspot. Although it was not always possible to discern whether the animals' eyes were open or closed while lying down, the frequency and patterns of movement while in the neutral state of attention suggested the animals were not sleeping. Finally, external stimuli in the form of vocalizations by other chimps or movement on the wing were minimal during the uptake period of each chimp, and responses to these stimuli were few in number and brief in duration (SI Table 1).

Imaging Results. ***Humans.*** Examination of the 5% most-active voxels in the average human PET image ($n = 8$) revealed a large area of activity in posterior medial cortices, spanning the posterior cingulate gyrus (BA 23 and 31), precuneus (BA 7 and 31), and cuneus (BA 17; Fig. 1*a*) (The unthresholded average human PET image ($n = 8$) is shown in SI Fig. 3*a*). A second large area of activity was found in the left dorsolateral, rostrolateral, and premotor frontal cortex (BA 6, 8, 9, 10, and 46), extending ventrally into Broca's area (BA 44 and 45; Fig. 1*b*). A smaller but still large area of activity was observed in right dorsolateral, rostrolateral, premotor, and frontal cortex (BA 6, 8, 9, 10, and 46), extending minimally into the right hemisphere homologue of Broca's area (BA 44; Fig. 1*b*). However, no activity was found within right BA 45 at this threshold. Dorsomedial PFC (BA 8, 9, and 32) also showed widespread activity at this threshold (Fig. 1*a*). In addition to the lateral frontal cortex, several brain regions showed stronger activation in the left vs. right hemisphere, including anterior insula, striatum, thalamus, ventral portion of the postcentral gyrus in the vicinity of the second somatosensory area (S2), superior temporal (BA 22), middle temporal (BA 21), angular (BA 39), and supramarginal (BA 40) gyri (SI Fig. 4). Analysis of overlap across individual subject images thresholded at 5% implicated a similar set of areas (Fig. 1*c*).

Chimpanzees. Comparison of the 5% most active voxels across individual chimpanzee subjects did not reveal any marked difference between the chimpanzee that was scanned in isolation (SI Fig. 5*a*) and the other four (SI Fig. 5 *b*–*e*). [The unthresholded average chimpanzee PET image ($n = 5$) is shown in SI Fig. 3*b*] In particular, the lack of amygdala activity in the isolated subject suggested he was not considerably more anxious than the others. Based on this evidence, all five scan were averaged. Examination of the 5% most active voxels in the average chimpanzee PET image ($n = 5$) revealed a large area of activity spanning both ventral and dorsal MPFC (FE, FDL, FDm, FC, and FB, the homologues of BA 10, 32, 9, 8, and 6, respectively; Fig. 2*a*). Prominent areas of activity also included posterior cingulate cortex (LC_1, the putative homologue of BA 31; Fig. 2*a*), and bilateral dorsolateral and rostrolateral PFC (FC, FD-delta, FE, and FDm, the homologues of BA 8, 46, 10, and 9, respectively; Fig. 2*b*). Other areas showing activity at this threshold included visual cortical areas OA, OB, and OC (BA 19, 18, and 17, respectively), as well as areas PF and PG (BA 40 and 39, respectively) in the inferior parietal lobe. Again, analysis of overlap across individual subject images thresholded at 5% implicated a similar set of areas (Fig. 2*c*).

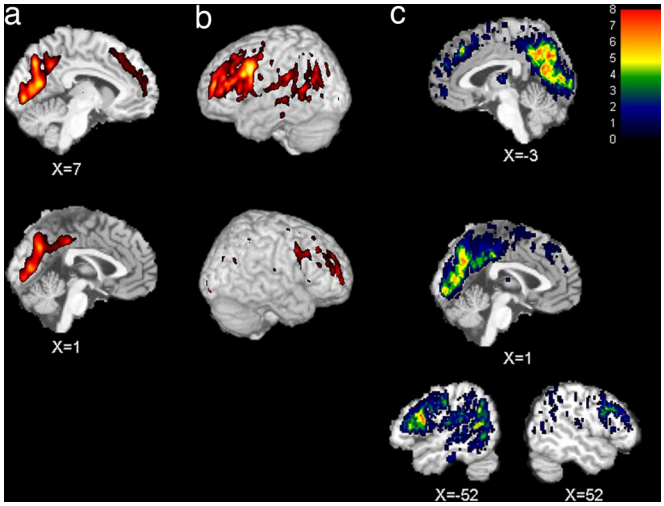

Fig. 1. Resting-state brain activity in humans. The five percent most active voxels in the average human brain ($n = 8$) displayed on midsagittal slices ($x = 1$ and $x = 7$) through the T1-weighted canonical brain from SPM (*a*) and left (*b Upper*) and right (*b Lower*) lateral surface reconstructions showing activity within 20 mm of the cortical surface. (*c*) Degree of overlap of 5% most active voxels across all eight human subjects shown on midsagittal slices ($x = -3$ and $x = 1$; top) and right and left parasagittal ($x = -52$ and $x = 52$; bottom) sections. *x* coordinates are given in millimeters from the midline.

Discussion

The brain areas that were most active at rest in our sample of human subjects overlap considerably with results of previous studies of resting-state brain activity. Using quantitative PET measures of blood flow and metabolism, Raichle *et al.* (5) showed that MPFC and medial parietal cortices have very high levels of activity at rest. High levels of activity in these regions were also found in the present study (Fig. 1*a*). MPFC and medial parietal cortex are also among the areas most consistently deactivated by attention-demanding cognitive tasks (4), an observation consistent with high levels of activity in these areas in resting baseline or low-level control conditions. MPFC and medial parietal cortex have been implicated in reflecting on the mental states of self and others (10, 11) and self-related episodic memory retrieval (7), respectively. Recently, it has been proposed that these regions constitute part of a more generalized network involved in mental self-projection, which includes thinking about the future (prospection), remembering the past, and conceiving the viewpoints of others (theory of mind) (20). The activity we observed in medial parietal cortex in humans extends

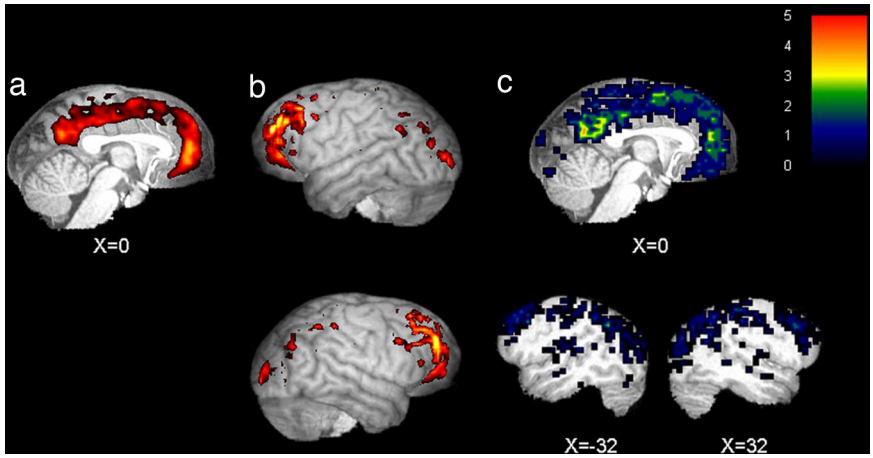

Fig. 2. Resting-state brain activity in chimpanzees. The five percent most active voxels in the average chimpanzee brain ($n = 5$) displayed on midsagittal slice through normalized T1-weighted brain from one chimpanzee (*a*) and left (*b Upper*) and right (*b Lower*) lateral surface reconstructions showing activity within 20 mm of the cortical surface. (*c*) Degree of overlap of the 5% most active voxels across all five chimpanzee subjects shown on midsagittal (*Upper*) and right and left parasagittal ($x = -32$ and $x = 32$; *Lower*) sections. *x* coordinates are given in millimeters from the midline.

posteriorly into visual cortex to a greater extent than observed by Raichle *et al.* (5). This is likely because our human subjects had their eyes open during the uptake period, whereas the subjects studied by Raichle *et al.* (5) had their eyes closed.

We also observed high levels of activity in lateral cortex in humans, including left posterior temporal and inferior parietal areas. This result is also consistent with previous studies reporting BA 39 (angular gyrus) to be more active at rest compared with various active task conditions (4, 8). These areas are involved in semantic knowledge retrieval (4, 8, 21). Binder *et al.* (8) argue they are part of a conceptual processing network that is active at rest in the human brain, linked to the occurrence of spontaneous thoughts and mind wandering, and deactivated by demanding external tasks. Indeed, activity was also observed in another node of this proposed conceptual processing network, namely dorsolateral and rostrolateral PFC, particularly in the left hemisphere, as has also been reported (2, 4, 8). However, the activity we observed was more widespread, extending lateral, posterior, and ventral to previously reported activations. In particular, earlier studies have not reported high levels of activity within the posterior portion of Broca's area (BA 44). However, the joint activity we observed within Wernicke's and Broca's areas is consistent with recent observations of functional connectivity between the two areas at rest (22).

In sum, the pattern of brain activity observed in our human subjects is similar to that reported in previous resting-state studies, and this pattern of activity is consistent with a resting state involving mentalizing, self-related episodic memory retrieval, conceptual and semantic processing, and inner speech.

Like humans, chimpanzees exhibited high levels of activity in MPFC and medial parietal cortices. Both species also exhibited high levels of activity in rostrolateral and dorsolateral PFC. However, there were also some noteworthy species differences. Within MPFC, humans showed the highest level of activity in more dorsal areas (BA 9, 32), whereas chimpanzees showed more widespread activity, including activity in more ventral areas (e.g., the homologue of human BA 10). Finally, the strongly left-lateralized activity related to language and conceptual processing in humans was absent in chimpanzees.

Analysis of the videotaped [^{18}F]-FDG uptake sessions suggested that the observed differences in brain activity between chimpanzees and humans were unlikely to be attributable to differences in activity or external stimulation. Chimpanzees were in a resting state throughout most of the brain uptake period. For the four chimpanzees from which we had complete video data, none interacted with their cagemate during the uptake phase, and all spent the majority of their time lying down or sitting in a neutral state of attention. Moreover, external stimuli (inferred from video and audio recordings of the uptake period), and particularly reactions to them, were rare.

This pattern of similarities and differences in resting-state brain activity may shed light on similarities and differences in resting-state cognition. The similarity in MPFC and medial parietal cortex activity at rest has interesting implications. First, if the MPFC activity uniquely relates to mentalizing about self or others, then chimpanzees must be capable of mentalizing. On the other hand, if the function of these regions is more general, as proposed by Buckner and colleagues (4), the results may imply that chimpanzees, like humans, are capable of mental self-projection. This possibility is supported by evidence that chimpanzees seem capable of imagining situations they cannot directly perceive (23). For example, a capacity to project into the past is suggested by chimpanzees' ability to indicate the location of a food reward hidden 16 hours earlier to a naïve observer (24), and a capacity to project into the future is suggested by the fact that they will transport tools for future use (25). A related possibility is that this region has overlapping functions in the two species (e.g., projecting into the future and the past), but that it has additionally evolved to take on theory-of-mind-related functions in humans but not chimpanzees. A similar process appears to have occurred in area 44, part of Broca's area in the inferior frontal gyrus: although area 44 has some shared functions in humans and non-human primates, including control of hand and orofacial movements as well as mirror neuron properties, only in humans does it have a role in speech articulation (26). Likewise, dorsomedial PFC activity at rest may have both common and distinct functions in humans and chimpanzees. Thus, although our results are not incompatible with chimpanzees exhibiting a theory of mind, they do not necessarily require this conclusion. Indeed, recent evidence for the existence of a default mode network in rhesus macaques (27), a species which most agree is incapable of theory of mind, suggests that theory-of-mind components were built by modifying preexisting systems that support cognitive functions present in a wide array of primate species.

Further evidence for potential similarity in resting-state cognition between humans and chimpanzees is provided by the fact that both species exhibit high levels of activity in rostrolateral PFC at the frontal pole (lateral BA 10). In humans, this region

is implicated in processing internally generated as opposed to externally generated information and in functions such as reasoning, working memory, and memory retrieval (28). If this region has a similar function in chimpanzees, our results could indicate that, like humans, chimpanzees are not constrained to thinking about what can be immediately perceived in the external environment but may instead generate thoughts internally that are unrelated to environmental inputs

Chimpanzees differed from humans in having stronger activity in ventromedial PFC. Recently, it has been suggested that different subdivisions of MPFC are related to different aspects of mentalizing (10, 29, 30), with more dorsal regions being involved with thinking about others' thoughts as well as person knowledge, and more ventral regions being involved with monitoring emotion in self and others or emotional processing more generally. Thus, it is possible that the chimpanzee resting state is imbued with a stronger emotional tone than the human resting state, perhaps including greater representation of emotional states as opposed to thoughts. However, given that other studies have found high levels of activity within ventromedial PFC in human subjects (5), it is possible that the lack of high levels of activity in this area in our human sample relates to differences in the exact nature of the resting-state condition rather than genuine species differences. For example, thinking about familiar and unfamiliar others has been localized to ventral and dorsal aspects of MPFC, respectively (30). That four of the five chimpanzees, unlike the humans, were surrounded by familiar others during the [^{18}F]-FDG PET uptake period could explain the higher levels of activity ventrally in chimpanzee images.

Unlike humans, chimpanzees did not show left-lateralized activity in frontal, temporal, and parietal regions. These results suggest that one major difference between humans and chimpanzees is that human resting-state cognition is linked with language. The left-lateralized areas that are active in humans but not in chimpanzees have also been implicated more generally in conceptual processing involving semantic knowledge retrieval, representation in awareness, and directed manipulation of represented knowledge for organization, problem-solving, and planning (8). Thus, organization, planning, and problem solving may be other aspects of resting-state cognition that differentiate humans from chimpanzees.

In conclusion, we find that, like humans, chimpanzees show high levels of resting-brain activity within default mode areas, including MPFC and posterior cingulate/precuneus. These results imply some degree of commonality in resting-state cognition. Although the results are consistent with the existence of theory of mind in chimpanzees, they do not require that conclusion, because homologous brain regions can evolve to take on different functions in different species (e.g., area 44). Chimpanzees differ from humans in showing higher levels of activity in ventromedial PFC and lower levels of activity in left-sided cortical areas involved in language and conceptual processing in humans. Our results raise the possibility that the resting state of chimpanzees involves emotionally laden episodic memory retrieval and some level of mental self-projection, albeit in the absence of language and conceptual processing.

Materials and Methods

Humans. ***Subjects.*** Study participants included eight healthy human subjects (six females) between the ages of 18 and 50.

PET image acquisition. PET scans took place at 11:00 a.m. All subjects fasted overnight and throughout the morning of the scan so that ingested glucose would not compete for neuronal uptake with ingested [^{18}F]-FDG. Seven of the eight subjects were scanned with an ECAT EXACT 921 PET camera (CTI Molecular Imaging, Knoxville, TN). The eighth was scanned with an ECAT EXACT 951 PET camera. These devices collect 31 (Siemens 951) or 47 (Siemens 921) contiguous 3.375-mm planes. After reconstruction, the resolution for both scanners is isotropic at 8 mm. The sensitivity is greater for the 921 scanner because of the extra detector ring, but counting statistics were not an issue in these studies (31). Each subject was placed in a dimly lit room adjacent to the PET scanner, and an i.v. line was inserted in the hand and warmed with a heating pad for measurement of arterialized venous blood samples. This method has been shown to yield metabolic values equivalent to those obtained by arterial line placement (32). The subject then received an i.v. injection of 10 mCi (1 Ci = 37 GBq) (370 MBq) of [^{18}F]-FDG in a single bolus. During the brain uptake period, subjects rested quietly in the dimly lit room. Twenty-three arterialized venous blood samples were obtained at multiple time points after injection for measurements of radioactivity in the plasma, which were used for construction of a plasma time activity curve for another study. Three blood samples were also obtained for measurement of plasma glucose concentrations. Samples were drawn by a research technician who did not converse with the subjects.

Between 45 and 65 min after injection, subjects were placed in the scanner with heads held in a head holder to minimize motion. The head was positioned with the canthomeatal line parallel to the external laser light. After positioning within the camera gantry, postinjection transmission data were collected by using rod windowing with three orbiting 67Ga/68Ge rod sources (31). These data were used to correct the emission data for attenuation because of overlying bone and soft tissue. The subject then underwent emission scanning of the brain with his or her eyes open in a dimly lit room. The scan duration was 20 min.

MRI acquisition. Structural MRI scans were acquired from all subjects for coregistration with the PET scans. MRI scans were obtained on a 1.5-T Philips Gyroscan Intera device (Philips Medical Systems, Andover, MS). T1-weighted images were acquired with a gradient echo 3D sequence with repetition time (TR) = 35 msec, echo time (TE) = 12 msec, flip angle = 35°, number of averages = 2, matrix = 256 × 256, field of view = 22 cm, and slice thickness = 3 mm. In addition, T2-weighted images were acquired with a turbo-spin echo sequence with TR = 4,400 ms, TE = 99 ms, flip angle = 163°, number of averages = 1, matrix = 256 × 256, field of view = 22 cm, slice thickness = 3.0 mm.

Partial volume correction. Given that human brains are approximately three times greater in volume than chimpanzee brains, human PET scans will have better anatomical resolution than chimpanzee PET scans, other things being equal. Although the high-resolution research tomograph scanner used for chimpanzee scans has higher spatial resolution than the ECAT camera that humans were scanned with, this is not sufficient to counter the difference in brain size. To equalize partial volume effects across species, a partial volume correction was implemented that theoretically corrects each PET scan to the resolution of the associated structural MRI scan (33, 34). T2-weighted scans were used for the partial volume correction, because they covered the entire brain, whereas T1-weighted scans did not.

Image analysis. Each subject's partial volume corrected PET scan was spatially coregistered to that individual's T1-weighted MRI scan in AC-PC orientation by using SPM2 (35). T1-weighted MRIs were then segmented into gray matter, white matter, and cerebrospinal fluid tissue probability maps. Each subject's T1 anatomical scan was then spatially normalized to the human T1-weighted MNI template in SPM2 (36), and this transformation was applied to the subject's PET scan and gray matter segment to warp them to MNI space. The spatially normalized gray matter images were smoothed with a 1.61-mm kernel. A binary mask was made of each subject's smoothed gray matter image, and all eight subjects' masks were multiplied together to create a common gray matter mask that included only voxels where every subject had gray matter. This common gray matter mask was applied to each subject's spatially normalized PET scan

to yield only the gray matter portion of the PET scan. All gray matter PET images were then normalized to the average activity of whole brain gray matter to facilitate comparisons of relative brain glucose metabolism across individuals and species. These images were averaged across all eight human subjects and then thresholded to display only the 5% most active voxels on top of the SPM canonical single subject T1 image (Fig. 1 *a* and *b*). Additionally, each individual's intensity normalized PET scan was thresholded to display only the 5% most active voxels. Binary masks were made of each subjects' thresholded image so that the 5% most-active voxels were assigned a value of 1, and the rest of the image was set to zero. These masks were summed to create an image showing the degree of overlap in the thresholded images of the eight subjects (Fig. 1*c*). Areas of high activity were assigned Brodmann's numbers based on comparison with Brodmann's map (37, 38).

Chimpanzees. ***Subjects.*** Five adult chimpanzees (two females) with a mean age of 19 years (range 13–29) were subjects for this study. For chimpanzees, this age corresponds to the young adult to middle-age period. Given suggestions that chimpanzees trained on symbolic tasks are cognitively different from other chimpanzees (39, 40), we note that, although these animals have been used in computer-based studies of social cognition, i.e., face recognition (41), they have had no formal language training, nor did any of the tasks involve symbolic representations.

PET image acquisition. Chimpanzees are typically pair-housed at the Yerkes National Primate Research Center. Initially, we planned to temporarily isolate chimpanzee subjects from their cagemates during the [^{18}F]-FDG uptake period to eliminate any possibility of social interactions that would disrupt the resting state. After 2 weeks of habituation to the procedure, the first chimpanzee subject was scanned in isolation. However, attempts to habituate subsequent chimpanzees to separation from their cagemates were unsuccessful, because animals showed sustained behavioral evidence of anxiety. Given prior observations that cagemates interact minimally for much of the day, we decided to conduct the remaining ($n = 4$) studies with the cagemate present, but at a time of day when animals interact minimally with either their cagemates or the animal care staff. This happened in the late morning hours. All subjects were food-deprived the morning of the scan, so that ingested glucose would not compete for neuronal uptake with ingested [^{18}F]-FDG. Each chimpanzee drank a dose of [^{18}F]-FDG ($\approx$15 mCi) in its home cage. A live video feed to a remote location was used to evaluate whether we had attained a resting state and abort a scan if necessary. Videotapes were later scored with an ethogram in 10-sec blocks to quantify the proportion of the uptake period that was spent resting (SI Table 1). One of six chimpanzee scans was aborted, because the live video feed showed that the subject was interacting with his cagemate. This scan was later successfully repeated on the same animal without any interaction.

Chimpanzees are highly attentive to the behavior of animal care staff. To minimize attention to external stimuli such as these and help facilitate a resting state, animals were tested in the late morning hours after animal care staff had completed their work and vacated the wing. Chimpanzees are also attentive to vocalizations of other chimpanzees living on the wing. These are typically minimal at this time of day but were also quantified from the audio that accompanied the videotape (SI Table 1).

A pilot study of [^{18}F]-FDG uptake after oral administration to anesthetized chimpanzees revealed that estimated brain uptake was 79% complete by 75 min after administration (L.A.P. and J.R.V., unpublished observation). Therefore, we waited 75 min after [^{18}F]-FDG administration before sedating animals with 5 mg/kg telazol. Subjects were then transported to the PET center and placed in the scanner, where they were given an i.v. bolus of 1–2 mg/kg propofol and maintained on an i.v. drip of propofol at 10 mg/kg per hour. Images were acquired with a Siemens High-Resolution Research Tomograph (CPS, Knoxville, TN) that has an approximate spatial resolution of 2.2 mm FWHM.

The head was positioned with the canthomeatal line parallel to the external laser light. After positioning within the camera gantry, postinjection transmission data were collected with a Cs-137 point source. An attenuation image was reconstructed, segmented into air, tissue (water), and bone, and the Cs-137 attenuation coefficients were replaced with the appropriate 511-keV attenuation coefficients. Attenuation correction factors were determined by foreprojecting this image.

The emission scan lasted 20 min. After the scan, the subject was transported back to its home cage to recover from anesthesia and monitored by veterinary staff. The subject remained alone for 24 h for radioactive decay of [^{18}F]-FDG and was then returned to its home cage.

MRI acquisition. MRI scans were acquired from all subjects for coregistration with the PET scans. Chimpanzee subjects were sedated with 5 mg/kg telazol and transported to a Siemens Trio 3T scanner. Before placing the animal in the scanner, an i.v. catheter was placed in the cephalic vein through which a propofol drip anesthetic (10 mg/kg per hour) was administered. A T1-weighted Magnetization Prepared Rapid Gradient Echo (MPRAGE) scan was acquired from each subject repetition time (TR) = 2,300 ms, echo time (TE) = 4.4 ms, inversion time (TI) = 1,100 ms, flip angle = 8, three signals averaged) with voxel sizes ranging from 0.60 mm isotropic to 1.0 mm isotropic. Scan duration ranged from 20 to 40 min.

Image analysis. As with human subjects, each chimpanzee subject's partial volume-corrected PET scan was spatially coregistered to that individual's T1-weighted MRI scan in AC-PC orientation by using SPM2 (35). T1-weighted MRIs were then segmented into gray matter, white matter, and cerebrospinal fluid. Each subject's T1 anatomical scan was then spatially normalized to a custom-made chimpanzee T1-weighted template (see below), and this transformation was applied to the subject's PET scan and gray matter segment to warp them to standard chimpanzee brain space. To create the chimpanzee template, a two-tiered procedure was used. First, MRIs from each of eight adult chimpanzees (five from the present study plus an additional three males) were placed in stereotactic orientation by using Analysis of Functional NeuroImage (45) software and then averaged together into a single image. Second, each individual MRI was spatially normalized to this average brain by using an affine transformation, and the eight normalized MRIs were finally averaged to create the standard.

Spatially normalized gray matter segments were smoothed with a 1.00-mm kernel. Kernel sizes for humans and chimpanzees were chosen such that their ratio matched the ratio of the linear dimensions of the brains of the two species. We computed a size factor $k = (Lx + Ly + Lz)/(lx + ly + lz)$, in which Lx is the distance between the brain extreme left and right points in humans; Ly, the distance between the brain extreme anterior and posterior in humans; Lz, the distance between the brain extreme inferior and superior in humans; lx, the distance between the brain extreme left and right points in chimpanzees; ly, the distance between the brain extreme anterior and posterior in chimpanzees; and lz, the distance between the brain extreme inferior and superior in chimpanzees and then multiplied the smoothing kernel size we selected for chimpanzees by k to arrive at the human smoothing kernel size of 1.61.

A binary mask was made of each subject's smoothed gray matter segment, and all five subjects' masks were multiplied together to create a common gray matter mask that included only voxels where every subject had gray matter. This common gray matter mask was applied to each subject's spatially normalized PET scan to yield only the gray matter portion of the PET scan. All gray matter PET images were then normalized to the average

activity of whole brain gray matter to facilitate comparisons of relative brain glucose metabolism across individuals and species. These images were averaged across all five chimpanzee subjects and then thresholded to display only the 5% most active voxels on top of a spatially normalized T1-weighted image from one of the five individual chimpanzees (Fig. 2 *a* and *b*). Additionally, each individual's intensity-normalized PET scan was thresholded to display only the 5% most active voxels. Masks were made of each subjects' thresholded image, so that the 5% most active voxels were assigned a value of 1, and the rest of the image was set to zero. These masks were summed to create an image showing the degree of overlap in the thresholded images of the five subjects (Fig. 2*c*). Areas of high activity were assigned numbers based on comparison with the map of Bailey *et al.* (42). Although Bailey *et al.* named areas according to conventions used in the human map of von Economo and Koskinas (43), that nomenclature can be readily translated into Brodmann's numbers (44) (for example, Bailey *et al.*'s area FCBm corresponds to BA 44).

We thank Dr. William Hopkins, Mr. Matthew Glasser, Ms. Sheila Sterk, Mr. Matt Heintz, and Dr. Mary Dent for assistance with various aspects of this study. Grant support was provided by the Center for Behavioral Neuroscience Science and Technology Center Program of the National Science Foundation under agreement no. IBN-9876754; National Institutes of Health (NIH)/National Center for Research Resources Grant RR-00165 to the Yerkes National Primate Research Center and NIH Grant R01-MH068791 (to L.A.P.).

1. Andreasen NC, O'Leary DS, Cizadlo T, Arndt S, Rezai K, Watkins GL, Ponto LL, Hichwa RD (1995) *Am J Psychiatry* 152:1576–1585.
2. Christoff K, Ream JM, Gabrieli JD (2004) *Cortex* 40:623–630.
3. Ingvar DH (1979) *Acta Neurol Scand* 60:12–25.
4. Shulman GL, Fiez JA, Corbetta M, Buckner RL, Miezin FM, Raichle ME, Petersen SE (1997) *J Cognit Neurosci* 9:648–663.
5. Raichle ME, MacLeod AM, Snyder AZ, Powers WJ, Gusnard DA, Shulman GL (2001) *Proc Natl Acad Sci USA* 98:676–682.
6. Gusnard DA, Raichle ME (2001) *Nat Rev Neurosci* 2:685–694.
7. Cavanna AE, Trimble MR (2006) *Brain* 129:564–583.
8. Binder JR, Frost JA, Hammeke TA, Bellgowan PS, Rao SM, Cox RW (1999) *J Cognit Neurosci* 11:80–95.
9. Bechara A, Damasio H, Damasio AR (2000) *Cereb Cortex* 10:295–307.
10. Amodio DM, Frith CD (2006) *Nat Rev Neurosci* 7:268–277.
11. Gallagher HL, Frith CD (2003) *Trends Cognit Sci* 7:77–83.
12. Fox MD, Snyder AZ, Vincent JL, Corbetta M, Van Essen DC, Raichle ME (2005) *Proc Natl Acad Sci USA* 102:9673–9678.
13. Fransson P (2005) *Hum Brain Mapp* 26:15–29.
14. Greicius MD, Krasnow B, Reiss AL, Menon V (2003) *Proc Natl Acad Sci USA* 100:253–258.
15. Gallup G (1970) *Science* 167:86–87.
16. Byrne RW, Whiten A (1992) *Man* 27:609–627.
17. Povinelli DJ, Bering JM, Giambrone S (2000) *Cognit Sci* 24:509–541.
18. Hare B, Call J, Tomasello M (2006) *Cognition* 101:495–514.
19. Phelps ME, Mazziotta JC (1985) *Science* 228:799–809.
20. Buckner RL, Carroll DC (2007) *Trends Cognit Sci* 11:49–57.
21. Price CJ (2000) *J Anat* 197:335–359.
22. Hampson M, Peterson BS, Skudlarski P, Gatenby JC, Gore JC (2002) *Hum Brain Mapp* 15:247–262.
23. Suddendorf T, Whiten A (2001) *Psychol Bull* 127:629–650.
24. Menzel CR (1999) *J Comp Psychol* 113:426–434.
25. Mulcahy NJ, Call J (2006) *Science* 312:1038–1040.
26. Preuss TM (2004) in *The Cognitive Neurosciences*, ed Gazzaniga MS (MIT Press, Cambridge, MA), 3rd Ed, pp 5–22.
27. Vincent JL, Patel GH, Fox MD, Snyder AZ, Baker JT, Essen DCV, Zempel JM, Snyder LH, Corbetta M, Raichle ME *Nature*, in press.
28. Christoff K, Ream JM, Geddes LP, Gabrieli JD (2003) *Behav Neurosci* 117:1161–1168.
29. Frith CD, Frith U (2006) *Neuron* 50:531–534.
30. Mitchell JP, Macrae CN, Banaji MR (2006) *Neuron* 50:655–663.
31. Weinhard K, Eriksson L, Grootoonk S, Casey M, Pietrzyk U, Heiss W (1992) *J Comput Assist Tomogr* 16:804–813.
32. Brownell G, Kearfott K, Kairento A-L, Elmaleh D, Alpert N, Correia J, Wechsler L, Ackerman R (1983) *J Comput Assist Tomogr* 7:919–924.
33. Meltzer CC, Leal JP, Mayberg HS, Wagner HN, Jr, Frost JJ (1990) *J Comput Assist Tomogr* 14:561–570.
34. Muller-Gartner HW, Links JM, Prince JL, Bryan RN, McVeigh E, Leal JP, Davatzikos C, Frost JJ (1992) *J Cereb Blood Flow Metab* 12:571–583.
35. Friston K, Ashburner J, Frith C, Poline J-B, Heather J, Frakowiak R (1995) *Hum Brain Mapp* 2:1–25.
36. Ashburner J, Friston KJ (1999) *Hum Brain Mapp* 7:254–266.
37. Brodmann K (1909) *Vergleichende Lokalisationslehre der Grosshirnrinde* (Barth, Leipzig, Germany).
38. Brodmann K (1912) *Anat Anz Suppl* 41:157–216.
39. Thompson RK, Oden DL, Boysen ST (1997) *J Exp Psychol Anim Behav Process* 23:31–43.
40. Parr LA, Waller BM, Vick SJ (2007) *Current Directions in Psychological Science* 16:117–122.
41. Parr LA, Winslow JT, Hopkins WD, de Waal FB (2000) *J Comp Psychol* 114:47–60.
42. Bailey P, Bonin Gv, McCulloch WS (1950) *The Isocortex of the Chimpanzee* (Univ of Illinois Press, Urbana, IL).
43. Economo C von, Koskinas G (1925) *Die Cytoarchitektonik der Hirnrinde des Erwachsenen Menschen* (Springer, Berlin).
44. Hassler R (1962) *Deutsche Med Wochenschr* 87:1180–1185.
45. Cox RW (1996) *Comput Biomed Res* 29:162–173.